Nucleic Acids Research, 1998, Vol. 26, No. 16 **3657–3666**

Assembly of MMTV promoter minichromosomes with positioned nucleosomes precludes NF1 access but not restriction enzyme cleavage

Patrizia Venditti, Luciano Di Croce, Manfred Kauer[+], Thiemo Blank[1], Peter B. Becker[1] and Miguel Beato*

IMT, Institut für Molekularbiologie und Tumorforschung, Marburg, Emil-Mannkopff-Straße 2, D-35033 Marburg, Germany and [1]EMBL, Meyerhofstraße 1, D-649117 Heidelberg, Germany

Received May 20, 1998; Revised and Accepted July 2, 1998

ABSTRACT

To generate long arrays of nucleosomes within a topologically defined chromatin domain we have assembled minichromosomes on negatively supercoiled plasmid DNA with extracts from *Drosophila* preblastoderm embryos. These minichromosomes are dynamic substrates for energy-dependent nucleosome remodeling machines that facilitate the binding of various transcription factors but do not exhibit nucleosome positioning. In contrast, if such minichromosomes include the mouse mammary tumour virus (MMTV) promoter we find it wrapped around a nucleosome with similar translational and rotational position as *in vivo*. This structure precluded binding of NF1 to its cognate site at –75/–65 at salt concentrations between 60 and 120 mM, even in the presence of ATP, which rendered the NF1 site accessible to the restriction enzyme *Hin*fI. However, insertion of 30 bp just upstream of the NF1 site, which moves the site to the linker DNA, allowed ATP-dependent binding of NF1 to a fraction of the minichromosomes, even in the presence of stoichiometric amounts of histone H1. The minichromosomes assembled in the *Drosophila* embryo extract reproduce important features of the native MMTV promoter chromatin and reveal differences in the ability of transcription factors and restriction enzymes to access their binding sites in positioned nucleosomes.

INTRODUCTION

The mouse mammary tumour virus (MMTV) promoter, located in the long terminal repeat (LTR) of the provirus, is induced by glucocorticoids and progestins. Hormonal induction is mediated by a complex hormone responsive region (HRR) comprising several binding sites for the hormone receptors, a binding site for NF1, and two binding sites for the ubiquitous factor OTF1 (1 and references therein). The binding sites for the hormone receptors are imperfect palindromes which function synergistically as hormone-responsive elements (HREs) *in vivo* (2). Moreover, mutation of the NF1 binding site reduces hormone induction by one order of magnitude, without affecting receptor binding to the HRR, and mutation of both octamer motifs also reduces induction, though to a lesser extent (1). Thus, binding of hormone receptors, NF1 and OTF1 to the HRR and synergism between the three factors is necessary to achieve full induction of the promoter. On the other hand, *in vitro* binding studies have demonstrated that NF1 competes with hormone receptor and OTF1 for binding to naked promoter DNA (3,4), excluding a simple cooperativity of DNA binding as an explanation of the functional synergism among the three sequence-specific transcription factors.

In metazoan and yeast cells carrying stable copies of the MMTV-LTR, the promoter is organized in positioned nucleosomes, though their precise translational positioning is still a matter of debate (5–8). In the majority of the published studies, the nucleosome originally identified as nucleosome B (5) spans the HRR. Genomic footprinting studies have shown that after glucocorticoid or progestin induction all *cis*-acting elements in the promoter are occupied, while the position of the nucleosome appears to remain unchanged (8). Thus, the MMTV promoter becomes transcriptionally competent and bound by the three sequence-specific factors, whereas the nucleosome covering the HRR is neither removed nor shifted. However, the central region of this regulatory nucleosome becomes highly accessible to double-strand cleavage by nucleases (8), suggesting that the nucleosome is remodelled to accommodate simultaneously all relevant transcription factors. An active role of nucleosomes in mediating hormonal induction is suggested by experiments in yeast strains manipulated to express the MMTV promoter under the control of glucocorticoids and NF1 (7). Lowering the density of nucleosomes in these yeast strains compromises the synergism between hormone receptors and NF1 and reduces the extent of

*To whom correspondence should be addressed. Tel: +49 6421 28 62 86; Fax: +49 6421 28 53 98; Email: beato@imt.uni-marburg.de

[+]Present address: Diabetes Forschung Institut, Auf'em Hennekamp 65, 40225 Düsseldorf, Germany

The authors wish it to be known that, in their opinion, the first two authors should be regarded as joint First Authors

MMTV induction (9). How this positive role of the nucleosome is brought about is unknown.

MMTV promoter sequences can be assembled with histone octamers *in vitro* to generate a positioned nucleosome with a similar rotational phase as found *in vivo* (10–13). In binding studies with reconstituted mononucleosomes, the hormone receptors are able to access some of the HREs (10,11), whereas NF1 cannot bind to its cognate sequence (11,13,14). Even after preincubation with hormone receptors, no binding of NF1 to a nucleosomally organized MMTV promoter is observed *in vitro* (11), suggesting that mechanisms or factors are operating *in vivo* which are not present or active in the purified mononucleosome.

Recently, ATP-dependent chromatin remodeling factors have been identified biochemically and genetically which may be involved in the transactivation of inducible genes. To this class belong members of the large SWI/SNF complex, originally found in yeast genetic screens (15). Homologues to the yeast SWI/SNF complex, in particular to SWI2/SNF2 subunit, have been found in *Drosophila*, mouse and human. These genes encode DNA-dependent ATPases the activity of which is essential for the function of the complex. *In vitro*, the SWI/SNF complex is able to influence the structure of nucleosomes and facilitates the binding of transcription factors to DNA sequences organized around histone octamers (16–18). Other activities related to, but distinct from, the SWI/SNF complex have been identified recently in *Drosophila* and yeast (19–22), suggesting that the eukaryotic cell devotes a diverse set of factors to negotiate the chromatin structure in the context of transcriptional gene activation (23).

Extracts from *Drosophila* embryos are known to assemble DNA into physiologically spaced nucleosome arrays (24,25) and have been shown to possess ATP-dependent chromatin remodeling activities (19,21,22,25–27). We have used such extracts for the assembly of minichromosomes on plasmids containing MMTV promoter sequences. Here we report the structural characterization of these minichromosomes, which exhibit positioned nucleosomes over the MMTV promoter. As a test for the functional relevance of the positioned nucleosomes, we analyze the accessibility of the nucleosomal NF1 binding site. In contrast with many other transcription factors and similar to the *in vivo* situation, NF1 is unable to bind to the nucleosomally assembled wild-type MMTV promoter sequences despite the presence of remodeling machines. However, we observe an ATP-dependent stimulation of NF1 binding to a site situated in a nucleosomal linker. In contrast with NF1, the restriction enzyme *Hin*fI can access the NF1 binding site in an ATP-dependent fashion, independent of its position within a nucleosome or in the linker DNA. Thus, NF1 binding to DNA within a positioned nucleosome requires chromatin remodeling events distinct from those mediating *Hin*fI cleavage.

MATERIALS AND METHODS

1,10-phenantroline-copper, sarcosyl, micrococcal nuclease (MNase), apyrase and ribonuclease A (RNase A) were obtained from Sigma. Desoxyribonuclease I (DNase I), *Hin*fI and T4 polynucleotide kinase were from Boehringer Mannheim. The Stoffel fragment of DNA polymerase was from Perkin Elmer.

Preparation of *Drosophila* embryo extracts and chromatin assembly reaction

Standard assembly reactions were performed essentially as described (28). Briefly, 750 ng of DNA were incubated for 6 h at 26°C in the presence of 40 µl of *Drosophila* preblastoderm embryo extract (conductivity equivalent to 80 mM KCl), 80 µl of extraction buffer-110 (110 mM KCl, 10 mM HEPES–KOH, pH 7.6, 1.5 mM $MgCl_2$, 0.5 mM EGTA) and 13.3 µl of an ATP regenerating system (30 mM creatin phosphate, 3 mM $MgCl_2$, 3 mM ATP, 1 µg/µl creatin phosphokinase, 1 mM DTT). The salt concentration under these standard conditions is 120 mM. Where indicated, salt concentration in the extraction buffer was adjusted to achieve an overall conductivity of 60, 90 and 150 mM.

Two-dimensional gel electrophoresis

After the assembly reaction, samples were treated with RNase A for 30 min, followed by overnight treatment with proteinase K and 0.2% SDS at 37°C, two phenol extractions, and ethanol precipitation. The resulting DNA was analyzed for topoisomers distribution in two-dimensional gel electrophoresis as described (29). In the first dimension, electrophoresis was on a 1% agarose gel run in 1× TBE buffer for 16 h at 50 V. The agarose slice containing the sample of interest was rotated 90° and run at 80 V for 20 h in the second dimension on a 1% agarose gel, 1× TBE containing 2 µg/ml chloroquine, which was also added to the running buffer. Chloroquine was eliminated by soaking the gel for 40 min in H_2O and topoisomers were visualized by ethidium bromide staining or Southern blot hybridization (30).

Low resolution analysis of chromatin structure

Copper-phenantroline cleavage. After the assembly reaction, samples were incubated with 1,10-phenantroline-copper (31) and RNase A for 15 min at 37°C, treated with proteinase K in 0.2% SDS at 37°C overnight, phenol extracted twice and ethanol precipitated. Samples were then treated with 3-mercaptopropionic acid (MPA), ethanol precipitated, resuspended in 30 µl of Tris–EDTA (10 mM Tris–HCl, pH 7.6, 1 mM EDTA-Na_2) and dried in the speed vac three times. The resuspended samples were restricted overnight with *Eco*RI, phenol extracted, ethanol precipitated and resolved on a 1.3% agarose gel. After electrophoresis the gel was blotted onto a Quiabrane nylon-plus membrane (Qiagen) and probed with a labeled *Eco*RI–*Bgl*II probe, a restriction fragment from the plasmid pMMTVCAT B-B spanning 263 nucleotides in the CAT region, immediately downstream of the MMTV promoter (Fig. 1A).

MPE. Standard reconstituted chromatin or naked DNA were diluted in CB buffer (15 mM Tris–HCl, pH 7.4, 60 mM KCl, 15 mM NaCl, 0.25 M sucrose). DTT and H_2O were added just before use to a final concentration of 2 mM each. Then, 0.1 vol of a 10-fold concentrated reaction mix [1 mM MPE and 1 mM $(NH_4)_2Fe(SO_4)_2.(H_2O)_6$ in CB buffer] was added and aliquots of each sample removed for analysis after 1, 5 or 10 min by stopping the reaction with 5 mM Bathophenantrolinedisulfonacid (Sigma) dissolved in H_2O, followed by two phenol extractions and ethanol precipitation (32). Restriction, electrophoresis and indirect end-labeling was as described above for copper-phenanthroline products.

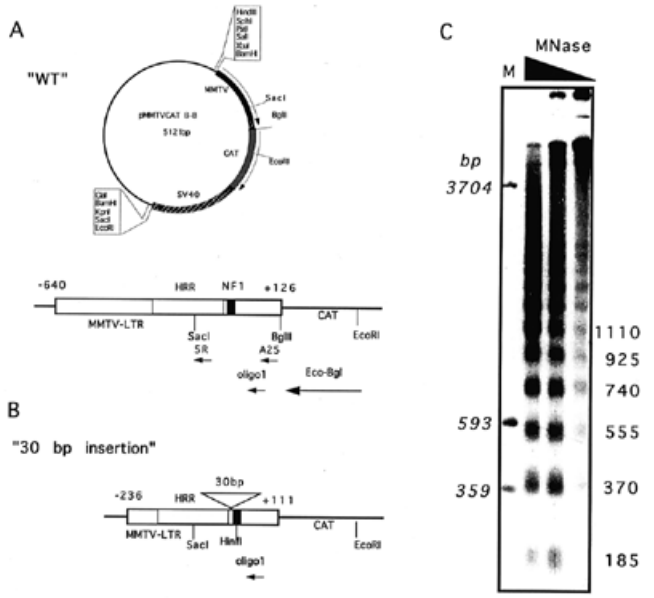

Figure 1. Assembly of chromatin on MMTV plasmids. (**A**) Schematic representation of the wild-type ('WT') MMTV plasmid, pMMTVCAT B-B, indicating the total number of base pairs, and the position of the MMTV LTR fragment and of the CAT and SV40 sequences. The scheme underneath the plasmid shows the Region of the MMTV-LTR included in this plasmid. HRR, hormone responsive region; NF1, NF1 binding site. Also indicated are the position of the oligos and the probes used for indirect end labeling or PCR amplification. The arrows indicate the elongation direction for the primers. Numbers refer to the start of transcription on the MMTV promoter. (**B**) Position of the 30 bp insertion between the HRR and the NF1 site (13) and the location of the *Hin*fI site. Other symbols are as in (A). (**C**) Determination of nucleosome spacing with MNase. Chromatin assembled on pMMTVCAT B-B DNA was digested with increasing amounts of MNase and the resulting DNA fragments were analyzed by Southern blotting after electrophoresis on a 1% agarose gel in 1× TBE buffer. The numbers on the left indicate the size of the markers (lane M) in base pairs. The numbers on the right give the average size of the cleavage products.

High resolution analysis of chromatin structure

MNase digestion. Digestion with MNase was performed as follows. After the assembly reaction, MNase and $CaCl_2$ were added to a final concentration of 3 U/µl and 2 mM, respectively, and the samples were incubated at 26°C for different times (ranging from 10 s to 5 min). The reactions were stopped by incubation with 0.1 vol of 100 mM EDTA, 2.5% sarcosyl, and RNase A (1 mg/ml) for 15 min at 37°C, followed by treatment with proteinase K (1 mg/ml) in 0.5% SDS at 37°C overnight. The samples were then phenol extracted twice and ethanol precipitated. For naked DNA controls, 1.5 µg of plasmid DNA was digested with 0.25–1 U/µl of MNase, phenol extracted, ethanol precipitated and used for PCR analysis.

DNase I digestion. After the minichromosome assembly, digestion with DNase I was performed at 26°C for different times. The amount of DNaseI required for appropriate digestion was determined empirically for each batch of enzyme. The reactions were stopped and processed as described above for MNase digested samples. For naked DNA controls 1.5 µg of plasmid DNA was digested for 1 min at 26°C with 20–40 U/µl of DNase I, phenol extracted, ethanol precipitated and used for PCR analysis.

Binding of recombinant NF1

Porcine NF1/CTF2 (33) was expressed in Sf9 insect cells infected with a baculovirus expression vector encoding an N-terminal histidine-tagged protein. Purification of NF1 from the cell extracts was achieved by chromatography on a Nickel column, and resulted in >80% pure protein as judged by SDS–PAGE (34).

Dimethyl sulphate footprinting. Dimethyl sulfate (DMS) footprinting was performed as described (2). Briefly, 10 ng of reconstituted chromatin were incubated at 26°C in the presence of increasing amount of NF1 in TGA 90 buffer (10 mM Tris–HCl, pH 7.6, 90 mM NaCl, 1 mM $MgCl_2$, 0.1 mM EDTA, 1 mM mercaptoethanol, 10% glycerol, 0.1 mg/ml BSA) and 3 µg of calf thymus DNA in a total volume of 100 µl. Modification was initiated by the addition of 0.5 µl of DMS. After 30 s the reaction was stopped by addition of 25 µl DMS stop mix (1.5 M Na-acetate, pH 7, 1 M β-mercaptoethanol, 250 µg/ml tRNA) for 15 s, and the samples were phenol extracted, ethanol precipitated and used for PCR analysis.

*Hin*fI accessibility assay

*Hin*fI digestion was performed at 26°C using 200 ng of chromatin DNA and 200 U of enzyme in 50 µl assembly reaction. Reactions were stopped with 20 mM EDTA and 0.5% sarcosyl and the samples were treated with RNase A and proteinase K. After ethanol precipitation, a second restriction enzyme cleavage was performed using *Dra*I and the DNA isolated. Twenty nanograms of DNA were used as template for linear PCR with oligonucleotide A25 as a primer (Fig. 1A) and the resulting products were analysed on a sequencing gel.

Linear PCR amplification

DNaseI or MNase-treated samples were used as templates in a 30-cycle linear PCR reaction with the radioactive labeled oligonucleotide primer A25 (AGGATAAGTGACGAGCGGAGACGGG) complementary to the region between +50 and +25 of the MMTV-LTR. For DMS footprinting analysis oligonucleotide 1 (AATGTTAGGACTGTTGCAAGTTTACTC), complementary to the region between +18 and –8 of the MMTV promoter was used. Oligonucleotide primers were phosphorylated with 100 µCi [^{32}P]ATP per 10 pmol of primer, using T4 polynucleotide kinase, and purified by electrophoresis in acrylamide gels. Primer extension reactions were performed with the Stoffel fragment of DNA polymerase as enzyme, using 300 000 c.p.m. of radiolabeled oligonucleotide and 10–20 ng of template DNA in a total volume of 50 µl. Amplified DNAs corresponding to chromatin and naked DNA samples were phenol extracted, ethanol precipitated and analyzed on 6% acrylamide gels. Dried gels were analysed using a PhosphorImager (Molecular Dynamics) and the ImageQuant software v3.0.

RESULTS

Full loading of an MMTV promoter plasmid with nucleosomes

The plasmid pMMTVCAT B-B encompassing the MMTV promoter region (Fig. 1A) (35) was used for assembly of minichromosomes using extracts prepared from *Drosophila melanogaster* preblastoderm embryos (24). We first tested whether the nucleosomes deposited into the plasmid were

properly spaced, by digesting the minichromosomes with MNase and separating the resulting DNA fragments in agarose gels. Up to 16 nucleosomes could be distinguished in the ethidium bromide stained gel (data not shown). The actual spacing over the MMTV promoter, determined by Southern blotting with a MMTV promoter oligonucleotide, was close to 185 ± 5 bp at 120 mM salt (Fig. 1C), suggesting a tightly packaged nucleosome array.

To quantitate the number of nucleosomes in each circular plasmid we counted the number of negative supercoiled topoisomers using two-dimensional gel electrophoresis. This analysis is based on the observation that each nucleosome assembled on a circular DNA molecule introduces a negative superhelical turn. The resulting topoisomers can be separated by electrophoresis in one-dimensional (36) or two-dimensional gels (29,30). The minichromosomes reconstituted in the *Drosophila* embryo extracts exhibited a distribution of topoisomers ranging from –22 to –29, centred around –26 (data not shown). Given the size of the plasmid (5121 bp) and a nucleosome spacing of 188 bp, this number of topoisomers corresponds to the expected value if the plasmid was fully loaded with histone octamers. These results suggest that a large proportion of the plasmid DNA is loaded with a full complement of regularly spaced nucleosomes in the *Drosophila* embryo extract.

Translational nucleosome positioning over the MMTV promoter

Nucleosome positioning can be defined by two parameters: the rotational phasing, which describes the relation between the nucleosome and the helical periodicity of the DNA, and the translational phasing, which describes the position of the nucleosome relative to a given point along the DNA molecule. The nucleosome B over the MMTV promoter, which covers the HRR, has been shown to exhibit preferential translational and rotational phasing in intact metazoan cells (5,6,8), in the yeast *Saccharomyces cerevisiae* (7), and when reconstituted into mononucleosomes *in vitro* (10–13). Therefore, we next tested whether this preferential nucleosome positioning could be reproduced in the *Drosophila* embryo extract. Various nucleolytic agents and analytical techniques were used to assay the structural organization of the reconstituted minichromosomes. Low resolution analysis was based on cleavage with Cu-phenantroline (31) or methidium-propyl-EDTA-Fe_{II} (MPE) (32), followed by indirect end labeling (37). These chemical nucleases were preferred to MNase, as they do not exhibit the strong sequence preference of the enzyme within the MMTV promoter. As expected, cleavage with Cu-phenantroline did not produce distinguishable bands on naked DNA (Fig. 2A, lane D). However, digestion of assembled minichromosomes generated a ladder of periodically spaced preferential cleavage sites revealing a whole array of translationally positioned nucleosomes (Fig. 2A). At this resolution, the nucleosome positions, as determined using as molecular weight markers a 100 bp DNA ladder and MMTV restriction fragments, were in good agreement with those mapped in living cells (5,8). In particular, the cleavage site for *Sac*I–*Sst*I, which is known to map close to the centre of nucleosome B *in vivo* (8), was also found between two preferentially cleaved regions (Fig. 2A, lane S). This similarity was confirmed in a direct comparison of the MPE digestion pattern obtained with reconstituted minichromosomes and with chromatin from BPV cells carrying episomally integrated MMTV sequences fused to the CAT gene (8) (Fig. 2B). In both cases, a similar ladder of preferentially cleaved regions was observed and the *Sac*I–*Sst*I site was found close to the centre of nucleosome B (Fig. 2B, lane S). Thus, the *Drosophila* embryo extracts assembled nucleosomes in a preferential translational frame similar to that found *in vivo*.

A high resolution mapping of the borders of nucleosome B in the minichromosomes was performed using MNase footprinting, as previously reported (7). A protected region was detectable extending from position –43 to approximately –190, corresponding to that previously established for the main population of nucleosome B *in vivo* (8). The proximal and distal parts of the footprint, from positions –65 to –43 and –190 to –170, respectively, were less clearly protected (Fig. 3), as previously reported for other positioned nucleosomes (38), leaving a central more clearly protected region of ~100 bp. The footprint was flanked by a cluster of strong hypersensitive sites between –43 and –37 and another hypersensitive site at –200 (Fig. 3), similar to those found in *S.cerevisiae* strains carrying MMTV promoter sequences (7), which likely correspond to the beginning of the linker DNA. Thus, the majority of the minichromosomes assembled in the *Drosophila* embryo extracts carry a nucleosome B over the MMTV promoter with the previously reported main translational phases.

Effect of salt and histone H1

The spacing of nucleosomes in minichromosomes assembled with *Drosophila* embryo extracts has been shown to increase with increasing salt concentration (39). We have confirmed these findings in respect to general spacing of nucleosomes with the MMTV containing plasmid, using three different hybridization probes located over the nucleosome B, over nucleosome A and over the CAT gene. The results were very similar if not identical with all three probes (data not shown). The spacing was 160 ± 5 bp at 60 mM, 170 ± 5 bp at 90 mM, 185 ± 5 bp at 120 mM, and 190 ± 5 bp at 150 mM salt. At this high salt concentration, however, digestion was more advanced and the individual bands may already represent trimmed degradation products.

Despite the changes in apparent nucleosome spacing at the various salt concentrations tested, the positioning of the nucleosome B over the MMTV promoter determined by MNase footprinting did not change significantly (data not shown). However, the pattern of nuclease cleavage was qualitatively influenced by the salt concentration. In minichromosomes assembled at 60 and 90 mM salt the cleavage pattern in the proximal linker DNA was more similar to the naked DNA pattern but still hypersensitive sites were detected in this region. At 150 mM salt the footprint was less evident suggesting that the nucleosomal structure is destabilized at this high ionic strength. Independent of the salt concentration in the assembly reaction, the strong preferential MNase cleavage sites observed with naked DNA at –84 and –100 were protected in minichromosomes, indicating that this region was covered by nucleosomes in all cases.

Another parameter that influences the nucleosome spacing is the presence of linker histone H1, which is absent from preblastoderm embryo extracts (39). To investigate the effects of histone H1 on the nucleosome structure, a chromatin assembly reaction was performed at 120 mM salt in the presence of stoichiometric amounts of this linker histone. As expected, the spacing of the resulting material was increased by 20 bp when compared with control reactions in the absence of linker histones (data not shown). The effect was similar with hybridization

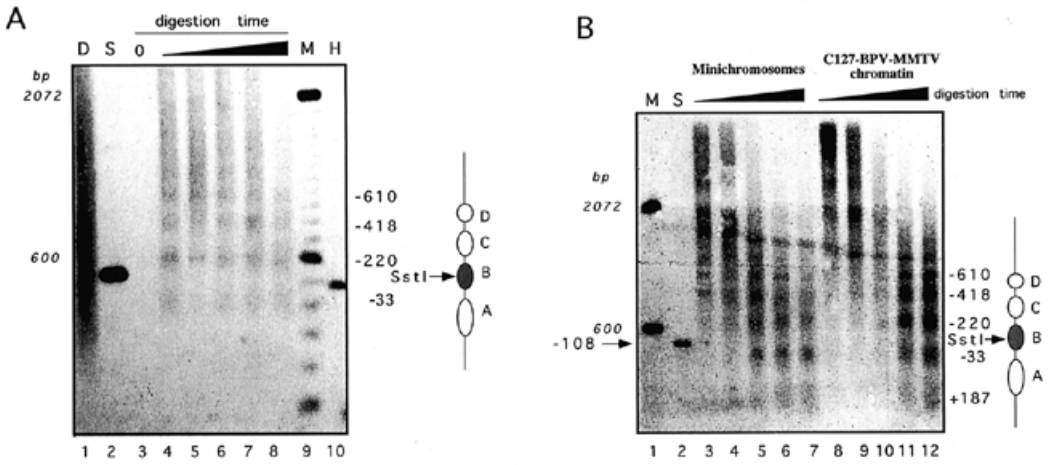

Figure 2. Low resolution mapping of nucleosomes positioning. (**A**) Minichromosomes were digested with Cu-phenantroline and the DNA products analyzed by indirect end labeling. Lane D, Cu-phenantroline reaction on naked DNA; lanes S and H, plasmid DNA restricted with *Eco*RI and with *Sac*I or *Hin*fI restriction enzymes, respectively; lane M, 100 bp ladder as molecular weight markers with two main fragments of 600 and 2072 bp; lanes 4–8, time course (0.5, 1, 2, 4 and 10 min) of the reaction on reconstituted minichromosomes. The nucleosomal ladder that appears upon addition of Cu-Phe MPA complex is indicative of translationally positioned nucleosomes with the nucleosomal linkers located at approximately –33, –220, –418 and –610. The scheme on the right margin shows the approximate positions of nucleosomes A, B, C and D. (**B**) MPE digestion pattern on *in vitro* reconstituted minichromosomes compared with digestion pattern obtained *in vivo* with C127-BPV-MMTV cells that carry 100–200 episomal copies of a BPV vector with MMTV promoter sequences linked to the CAT gene (8). To permit a direct comparison of the digestion products, chromatin from control C127 cells was added to the minichromosomes (lanes 3–7) prior to MPE digestion. The DNA products were analyzed by indirect end labeling with the *Eco*RI–*Bgl*II probe shown in Figure 1A. Lane M, two restriction fragments of 600 and 2072 bp as size markers; lane S, plasmid DNA restricted with *Eco*RI and with *Sac*I; lanes 3–7, time course of the digestion of minichromosomes mixed with C127 chromatin; lanes 8–12, time course of the digestion of chromatin from C127-BPV-MMTV cells. The inclined band extending from ~2000 on lanes 3 and 4 to –800 on lanes 10–12 is likely an artefact, which does not influence our calculation of the nucleosome positioning between –610 and +187. Numbers and the scheme on the right margin are as in (A).

probes corresponding to either nucleosome B, nucleosome A or to the CAT gene. However, a high resolution analysis of the translational position of nucleosome B did not reveal significant structural differences attributable to the presence of histone H1. In particular, the strong cleavage sites at –84 and –100 were protected in minichromosomes, and hypersensitive sites were found in the proximal linker DNA region. Thus, despite the effects on the apparent nucleosome spacing, addition of histone H1 did not change the preference of nucleosome B for the translational phases previously found *in vivo*.

Rotational phasing of the nucleosomes over the MMTV promoter

To analyze the rotational orientation of the double helix on the surface of the *in vitro* assembled nucleosome B we used DNaseI digestion, which should yield a pattern of preferential cleavage sites spaced by ~10 bp if a dominant rotational phase is present (11). The results shown in Figure 4 show a pattern of cleavage sites (indicated by arrows) spaced by ~10 bp, as previously found *in vivo* (8) and in *in vitro* assembled mononucleosomes (11). This pattern alternates with protection of cleavage sites (indicated by circles), which has also been observed in previous reconstitution experiments (11). Protections and enhancements in the DNase I cleavage of chromatin compared with free DNA are present also further downstream, but the 10 bp periodicity starts with a strong enhancement at position –42 followed by enhancements at –51/–53 and protections at –57/–59 and –66. Positions –73, –81, –91, –101, –112, –121, –132, –145 and –155 are either enhanced or preferentially recognized by DNaseI, while several positions in between are protected. We conclude that the MMTV promoter sequences in minichromosomes adopt a dominant rotational setting on nucleosome B, likely determined by the torsional anisotropy of the nucleotide sequence (40).

NF1 does not bind to the MMTV promoter assembled in minichromosomes

The dynamic properties of the *Drosophila* assembly system allow a variety of transcription factors to access their binding sites in chromatin (26,41–43). However, in previous studies nucleosomes were not positioned with respect to the underlying DNA sequence. We and others have previously shown with reconstituted mononucleosomes, that the inclusion of the NF1 binding site within the limits of a nucleosome precludes (11,13,14) or drastically inhibits (44) binding of NF1 *in vitro*. We therefore tested whether the positioned nucleosomes reconstituted in the context of a nucleosomal array with dynamic properties would also prevent NF1 from interacting with its binding site. Using DMS genomic footprinting we detected binding of histidine-tagged recombinant NF1 to the MMTV promoter on free DNA, but failed to observe protection over the NF1 site in promoters assembled into minichromosomes (Fig. 5A, compare lanes 4 and 7). These experiments were performed in the presence of ATP, suggesting that the NF1 binding site was not exposed for protein binding under conditions that allow functioning of the remodeling activities present in the *Drosophila* embryo extracts (42). To test whether components of the assembly reaction were responsible for the lack of binding of NF1, we allowed NF1 to bind to free MMTV DNA in the presence of the assembly extract but without allowing chromatin reconstitution to take place. Under these conditions, we did not observe an inhibition of NF1 binding (data not shown).

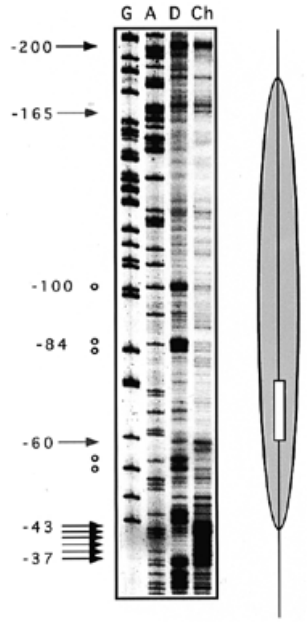

Figure 3. High resolution mapping of the translational positioning of nucleosome B. Minichromosomes reconstituted at 120 mM salt were mildly digested with MNase (20 s at 26°C) and the digestion pattern was visualized in a linear amplification reaction with oligonucleotide A25 (Fig. 1A). Lanes G and A, guanine and adenine specific sequencing reactions; lane D, MNase digestion pattern on naked DNA; lane Ch, chromatin sample treated with MNase. Cleavage sites protected in chromatin are indicated by open circles; hypersensitive sites are marked by black arrows. The region between the grey arrows (–60 to –165) is more clearly protected in chromatin. The numbers refer to the distance from the start of transcription. The diagram on the right shows the approximate position of nucleosome B. The location of the NF1 binding site is indicated by a white box.

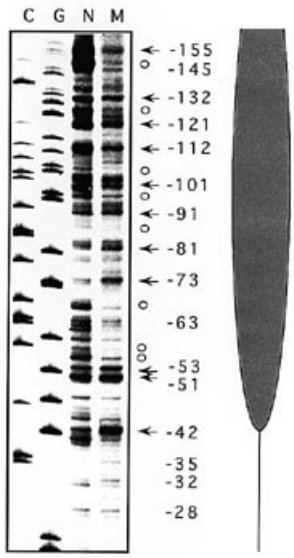

Figure 4. Rotational phasing of nucleosome B. The rotational setting of nucleosome B was determined by DNase I digestion of the minichromosomes followed by linear amplification (see Material and Methods). Lanes C and G, cytosine and guanine specific sequencing reactions; lane N: DNase I digestion pattern on naked DNA; lane M: minichromosomes digested for 5 min with DNase I. The alternate preferentially cleaved (arrows) and protected sites (circles) with ~10 bp periodicity are indicated. The numbers refer to the distance from the transcription start site. The scheme on the right shows the position of nucleosome B as determined by MNase footprinting (Fig. 3).

These unexpected results suggest that, in contrast with all previously reported data with *Drosophila* extracts, the NF1 binding site over the MMTV promoter remains inaccessible for the histidine-tagged recombinant NF1 when the promoter is organized in nucleosomes. To test whether the lack of binding of NF1 to the MMTV promoter in minichromosomes reflects a property of the recombinant protein or rather a general inaccessibility of the target sequence due to a positioned nucleosome, we performed experiments with restriction enzymes and with promoter mutations designed to alter nucleosome positioning.

The restriction enzyme *Hin*fI can access the NF1 site on the MMTV minichromosomes in the presence of ATP

The upstream half of the NF1 binding site within the MMTV promoter includes the recognition sequence for the restriction enzyme *Hin*fI, GAATC. This allowed us to compare the ability of *Hin*fI to cleave the MMTV promoter in mock assembled minichromosomes and in minichromosomes with positioned nucleosomes over the promoter. In addition, to test whether cleavage was ATP dependent, we performed the reaction in the presence or absence of apyrase, which degrades any ATP in the extract (26). The time kinetics of cleavage shows that whereas mock assembled promoter DNA was cleaved with equal efficiency in the presence or absence of apyrase, the promoter assembled in minichromosomes was efficiently cleaved only in the absence of apyrase (Fig. 5B). Thus, the NF1 binding sequences are accessible for restriction enzyme cleavage when positioned within a nucleosome, provided that ATP is available, which demonstrates that nucleosome B can in principle be the substrate for remodeling machines like CHRAC (21). We conclude that the inability of NF1 to access its binding site in minichromosomes likely reflects the specific nature of its interaction with DNA (13).

Moving the NF1 site to the nucleosomal linker allows ATP-dependent NF1 binding to minichromosomes

It is possible that the assembly of the MMTV promoter in minichromosomes creates a topological conformation of DNA incompatible with the NF1 binding independent of precise nucleosome positioning. To test this possibility we reconstituted minichromosomes into a plasmid carrying a 30 bp insertion between the HREs and the NF1 site (Fig. 1A). We have previously shown in mononucleosome assembly reactions, that this insertion moves the NF1 site to the linker region downstream of nucleosome B (13). In contrast with the results with the wild-type MMTV, we did detect DMS protection over the relevant guanines of the NF1 binding site with minichromosome reconstituted on the 30 bp insertion mutant (Fig. 6A). The protection, however, was 50% of that found in free promoter DNA, suggesting that binding to the NF1 site in the minichromosomes with the 30 bp insertions is still restricted to some extent. This could be due to the heterogeneity of the nucleosomal organization of promoters containing this insertion (13), as high resolution analysis of the translational positioning of nucleosome B revealed that only in 50% of minichromosomes was the NF1 site located in the linker region (data not shown). Moreover, binding to the 30 bp insertion mutant

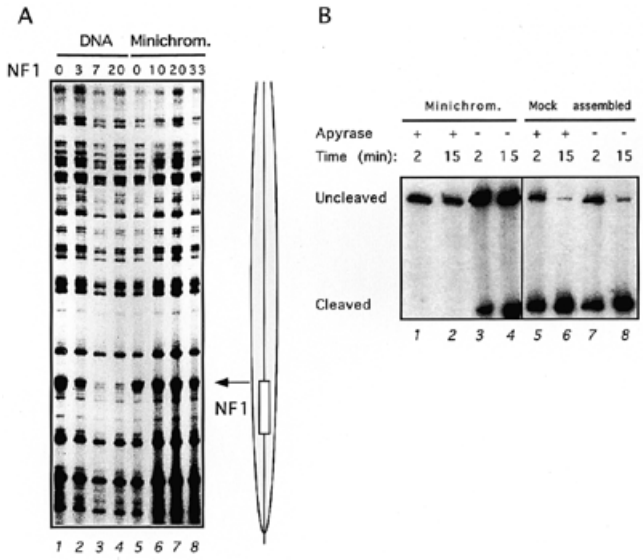

Figure 5. Access of NF1 and *Hin*fI to the wild-type MMTV promoter in minichromosomes. (**A**) Binding of NF1 as assayed by DMS footprinting. Naked DNA and reconstituted chromatin (corresponding to 10 ng DNA) were incubated with recombinant NF1 for 30 min at 26°C in the presence of 1 mM ATP and subjected to DMS footprinting. The amount of NF1 (ng) added is indicated above each lane. The guanine residues contacted by NF1 are indicated by an arrow. The scheme on the right shows the position of nucleosome B and the NF1 site. (**B**) Digestion with *Hin*fI. MMTV minichromosomes (200 ng DNA) were assembled as described in Materials and Methods, or with heat inactivated (80°C for 10 min) *Drosophila* embryo extract to yield the mock assembled control. During the last 10 min of the assembly reaction the samples were divided in two halves. One half was treated with apyrase (4 U) at 26°C and the other half served as a control. After assembly, the samples were digested at 26°C with 100 U of *Hin*fI for the indicated times, and the DNA was purified and restricted with *Dra*I. The digestion products were analyzed by linear PCR using oligonucleotide A25 (Fig. 1A). The positions of the *Hin*fI uncleaved and cleaved fragments are indicated.

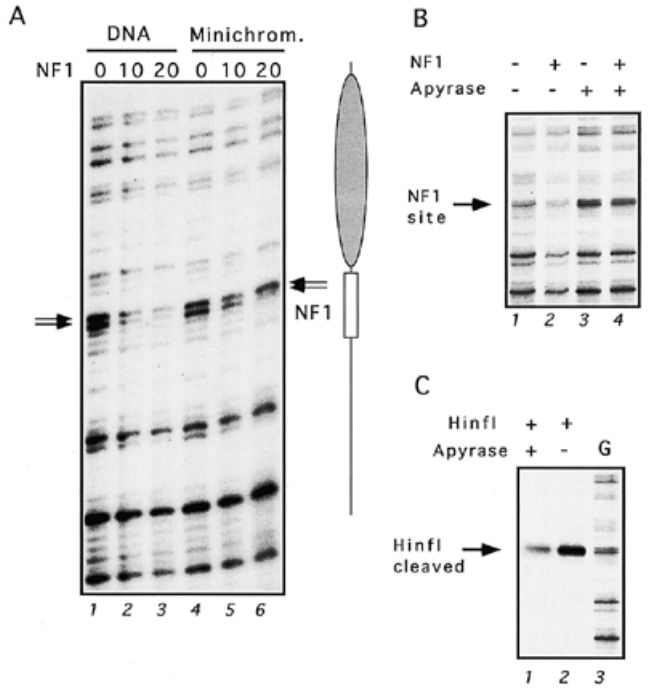

Figure 6. Access of NF1 and *Hin*fI to the 30 bp insertion mutant in minichromosomes. (**A**) Binding of NF1 as assayed by DMS footprinting. Experimental conditions were as described in Figure 5A but using a plasmid with the 30 bp insertion mutant of the MMTV promoter. Quantitation using a PhosphorImager showed that the average protection of the NF1 site (indicated by two arrows) in minichromosomes was 50% of that found with naked DNA (average of the results obtained with 10 and 20 ng of NF1). The scheme on the right shows the expected position of nucleosome B and the NF1 binding site. (**B**) Effect of apyrase on NF1 binding. DMS footprinting analysis was performed as in (A), but two samples were incubated in the presence of apyrase (4 U) as described in the legend to Figure 5B. The position of the guanines contacted by NF1 are indicated by an arrow. Only a narrow window of the sequencing gels is shown and the gel was run for a shorter time than in A. (**C**) Cleavage by *Hin*fI. The reactions were performed as in Figure 5B, except that incubation with *Hin*fI was for 2 min. Lane G, guanine specific sequencing reaction. The position of the *Hin*fI cleavage products are indicated by an arrow.

was dependent on ATP, since we did not observe NF1 binding if apyrase was included in the reaction (Fig. 6B). As expected, cleavage by the restriction enzyme *Hin*fI of the minichromosomes carrying the 30 bp insertion mutant of the MMTV promoter was also reduced in the presence of apyrase (Fig. 6C). We conclude that, while the chromatin remodeling activities present in the *Drosophila* extract are sufficient to mediate access of NF1 to its target sequences located on linker DNA, they cannot facilitate binding of histidine-tagged recombinant NF1 to a site located over a positioned nucleosome.

NF1 binding to the 30 bp insertion mutant is not influenced by histone H1

Having shown that a fraction of the minichromosomes carrying the NF1 binding site in the linker between nucleosomes B and A was able to bind histidine-tagged recombinant NF1, the question arose of whether this binding would be influenced by addition of linker histones, which are supposed to contact linker DNA (45). To test this we incorporated histone H1 into the minichromosome assembly reaction in amounts that generate an increase in nucleosome spacing of 20 bp (data not shown), and performed DMS footprinting experiments with and without recombinant NF1 (Fig. 7). The results show that, in the presence of ATP, NF1 is able to bind to the H1-containing minichromosomes with an affinity comparable with those lacking linker histones. In the absence of histone H1, protection of the guanine doublet over the NF1 site was 71%, whereas in its presence it was 47% as quantitated with a PhosphorImager (Fig. 7). Thus, incorporation of histone H1 into the minichromosomes slightly reduced but did not preclude binding of NF1 to its cognate within linker DNA.

DISCUSSION

Reconstruction of MMTV promoter chromatin structure in minichromosomes

The aim of this work was to recreate the well characterized *in vivo* chromatin organization of MMTV promoter sequences in a cell-free system, capable of generating long nucleosomal arrays under physiological conditions. To this end, we used extracts from *Drosophila* preblastoderm embryos (24). However, previous attempts to positioned nucleosomes using the well-known 5S rDNA derived positioning elements in the dynamic *Drosophila* assembly system were unsuccessful (46). Successful nucleosome positioning involved sequence-specific binding protein that served as boundaries for the statistical positioning of nucleosomes (27,43;

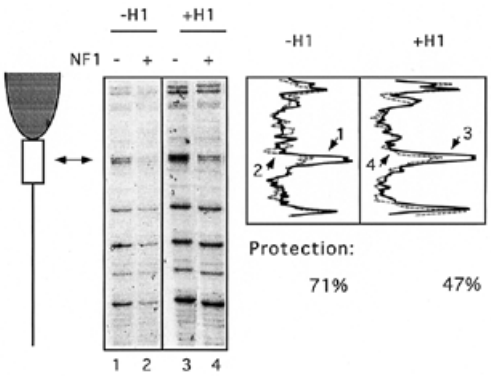

Figure 7. Influence of histone H1 on NF1 binding to MMTV minichromosomes carrying the 30 bp insertion. Minichromosome assembly reactions were performed with a plasmid containing the MMTV 30 bp insertion mutant, in the absence of added linker histones or in the presence of stoichiometric amounts of histone H1 (1 molecule per nucleosome). Binding of NF1 (20 ng) was measured by DMS footprinting as indicated in the legend of Figure 5A. Left, autoradiogram of the sequencing gel. The two guanines protected by NF1 are indicated by an arrow. The predicted position of nucleosome B and the NF1 binding site are shown on the left margin. Right, PhosphorImager quantitation of the extent of protection. Only the scans around the NF1 site are shown. The numbers indicate the corresponding lanes. The percentage protection in the presence of NF1 is indicated.

E.Bonty and P.B.Becker, unpublished observations). In contrast, when assembled in the *Drosophila* system as part of a long array of nucleosomes, nucleosome B, which covers the hormone regulatory region of the MMTV promoter *in vivo*, showed the same dominant translational and rotational phases previously found in metazoan and yeast cells. The similarity of the nucleosomal organization *in vivo* and *in vitro* is demonstrated at low resolution by comparing the MPE digestion patterns of the minichromosomes assembled *in vitro* and of chromatin from cells carrying episomal copies of the MMTV promoter (8). The translational positioning of nucleosome B was confirmed by high resolution footprinting with MNase, and the dominant rotational phase was established by the preferential cleavage of DNase I. Our analysis does not distinguish between a single translational frame and two adjacent frames with the same rotational orientation (47). We conclude that the MMTV promoter contains sequences particularly suited to direct nucleosomal positions.

Salt and histone H1 do not change the footprint of nucleosome B

The nucleosome repeat length of chromatin reconstituted in extracts varies as a function of the ionic conditions (39). The preferential positioning of MMTV nucleosome B, determined by MNase footprinting, was not altered when the nucleosome repeat length of the array was altered by varying the salt concentration in the assembly reaction between 60 and 120 mM. This indicates a dominant influence of the underlying sequence, an interesting contrast with experiments using the 5S rDNA positioning element (46). It remains to be established whether the position of other nucleosomes within the minichromosomes is dependent on salt concentration.

The role of linker histone H1 in regulation of the MMTV promoter is unclear. Although the MMTV promoter is regulated normally when introduced in *S.cerevisiae*, which supposedly lacks linker histones (7), an interaction of histone H1 with NF1 recognition sites has been suggested (48), and a relative depletion of histone H1 has been described following hormone induction (49). Since extracts from *Drosophila* preblastoderm embryo are devoid of histone H1 and we observed the same nucleosome positioning as in mammary cells, it seems that histone H1 does not play an essential role in determining the position of the nucleosomes in the MMTV promoter. Nevertheless, we tested the effect of adding exogenous histone H1 on the chromatin structure of the MMTV promoter. As expected (39), addition of stoichiometric amounts of histone H1 during the chromatin assembly reaction led to an increase in spacing of 20 bp no matter whether the probe used for Southern analysis corresponded to nucleosome B or to other regions of the plasmid. However, there was no significant difference in the high-resolution MNase footprint generated by nucleosome B, in particular concerning the proximal border of the nucleosome. These results confirm the lack of influence of this linker histone on the translational positioning of nucleosome B (7) and support a strong dominant role of the underlying DNA sequence.

ATP-dependent chromatin remodeling is not sufficient for NF1 binding to nucleosome B but enables access of *Hin*fI to the NF1 site

In agreement with previous results with mononucleosomes reconstituted by salt dialysis we could not detect binding of recombinant NF1 to the MMTV promoter assembled in mini-chromosomes (11,13). The lack of binding was observed in the presence of concentrations of ATP that support the function of the remodeling activities in the *Drosophila* embryo extract. This lack of NF1 binding in the presence of ATP is in contrast with the behavior of other transcription factors, such as the GAGA factor (26,41), heat shock factor (42), TTF1 (43), and Gal4 derivatives (27),which are able to bind to minichromosomes containing the corresponding cognate sites. The lack of binding is not due to inhibitory factors in the extract, since NF1 binding to naked DNA was not affected by addition of the *Drosophila* embryo extract in the absence of chromatin assembly. The discrepancy with other previously studied promoters in minichromosomes likely reflects the preferential positioning of nucleosome B, since in previous systems nucleosomes were not translationally positioned and the location of nucleosomes was more dependent on ionic strength and DNA topology than on DNA sequence (46). We hypothesize that the observed inability of NF1 to interact with nucleosomal binding sites may either be due to a particular sensitivity of the factor to nucleosomal inhibition and/or to the increased resistance of well-positioned nucleosomes to remodeling processes.

This interpretation is supported by the results obtained with the 30 bp insertion mutant, in which the NF1 binding site is exposed in the proximal linker of nucleosome B (13). Although the exact nucleosome structure of this mutant promoter in minichromosomes is heterogeneous, binding of NF1 to a significant fraction of the promoters is observed. This binding was dependent on ATP, likely reflecting the requirement for chromatin remodeling activities present in the extract. Thus, accessibility to the linker DNA adjacent to a positioned nucleosome is an energy dependent process in minichromosomes, whereas it takes place in the absence of ATP in reconstituted mononucleosomes (13). This finding suggests that NF1 access to the linker DNA in the minichromosomes may be restricted by a higher order structure

of the nucleosome array, which must be overcome in an ATP-dependent process.

Incorporation of histone H1 into the minichromosomes, as demonstrated by the 20 bp increase in nucleosome spacing, did not preclude NF1 binding to the nucleosomal linker in the 30 bp insertion mutant. We have not mapped the exact contacts between histone H1 and the MMTV promoter, but our results are compatible with a recent model proposing an asymmetric binding of linker histones within the gyres of the nucleosome (50–52).

In contrast with NF1, the restriction enzyme *Hin*fI can access the NF1 binding site in minichromosomes in the presence of ATP, independent of whether the site is located within the positioned nucleosome B or in the adjacent linker DNA. It seems, therefore, that access of restriction nucleases to chromatin is not equivalent to binding of sequence-specific transcription factors. This difference may reflect the different methods used to detect binding of restriction enzymes and of high affinity transcription factors. Each time a restriction enzyme contacts its target sequence on DNA it generates a cleavage that can be subsequently detected as a positive signal in the linear PCR analysis. In contrast, binding of NF1 is measured by DMS methylation protection, and requires that a significant fraction of the recognition sequences is occupied at a particular time point to generate a negative signal, a footprint, in the PCR analysis. It is also possible that the different ways in which restriction enzymes and high affinity transcription factors contact DNA determine the differential binding to nucleosomally organized sequences (53). Whereas *Hin*fI contacts only 5 bp, GAATC, over one-half of the palindromic NF1 site, NF1 contacts 5 bp in each half of the palindrome which are separated by 5 bp (13). It remains to be established whether this behavior is a peculiarity of the recombinant histidine-tagged NF1 or reflects a more general binding behavior of transcription factors when faced with translationally positioned nucleosomes.

Our findings are compatible with the notion that positioned nucleosomes contribute to transcriptional repression of the MMTV promoter in the absence of hormone. They also have implications for the mechanism of hormonal induction of the MMTV promoter in chromatin. It seems that the ubiquitously available ATP-dependent chromatin remodeling activities were not sufficient to facilitate binding of NF1. Nucleosome remodeling has to be initiated or targeted by steroid hormone receptors. In contrast with NF1, steroid hormone receptors are able to interact with their cognate sequence when these are properly oriented in the surface of a positioned nucleosome (10,11,54,55) and could, therefore, recruit chromatin remodeling complexes. The SWI/SNF complex (56) is a likely candidate, as components of the complex have been shown to interact with the steroid hormone receptors (57–59) and the SWI/SNF complex seems to be required for optimal hormonal induction of target genes *in vivo* (58). The glucocorticoid receptor, but not NF1, has been shown to stimulate the nucleosome-disrupting activity of the partially purified SWI/SNF complex on mononucleosomes carrying an artificial HRE (18). Thus, the SWI/SNF complex, or other related remodeling activities, could alter the conformation of nucleosome B making the NF1 site accessible for protein binding. A possible mechanism could involve dissociation of histone H2A/H2B dimers (15,17), as NF1 has been shown to bind rather efficiently to the MMTV promoter positioned on a tetramer of histones H3 and H4 (47).

Alternatively, histone acetylation could be involved in hormone receptor-dependent chromatin remodeling. Steroid receptors have been shown to recruit co-activators, such as CBP/p300 (60,61) and SRC-1 (62), which either exhibit histone acetyltransferase activity (63,64) or are able to recruit further histone acetylating proteins, such as P/CAF (65). In line with this notion, partial inhibition of histone deacetylases by trichostatin A activates the MMTV promoter *in vivo* in the absence of hormone and potentiates hormone-dependent induction (66). However, direct evidence for a change in histone acetylation following hormone induction is still unavailable. The MMTV minichromosomes assembled in the *Drosophila* embryo extracts represent an additional tool for studying these processes *in vitro*.

ACKNOWLEDGEMENTS

We thank Bernhard Gross and Hannes Westphal, IMT, for providing purified recombinant NF1, and Jörg Klug for carefully reading the manuscript. P.V. and L.D.C. were postdoctoral fellows of the Cenci-Bolognetti Foundation. M.K. was a predoctoral fellow of the Graduierten Kolleg 'Tumorbiologie'. The experimental work was supported by grants from the European Union, the Deutsche Forschungsgemeinschaft and the Fonds der Chemischen Industrie.

REFERENCES

1 Truss,M. and Beato,M. (1993) *Endocrinol. Rev.*, **14**, 459–479.
2 Chalepakis,G., Arnemann,J., Slater,E.P., Brüller,H., Gross,B. and Beato,M. (1988) *Cell*, **53**, 371–382.
3 Brüggemeier,U., Rogge,L., Winnacker,E.L. and Beato,M. (1990) *EMBO J.*, **9**, 2233–2239.
4 Möws,C., Preiss,T., Slater,E.P., Cao,X., Verrijzer,C.P., van der Vliet,P. and Beato,M. (1994) *J. Steroid Biochem. Mol. Biol.*, **51**, 21–32.
5 Richard-Foy,H. and Hager,G.L. (1987) *EMBO J.*, **6**, 2321–2328.
6 Fragoso,G., John,S., Roberts,M.S. and Hager,G.L. (1995) *Genes Dev.*, **9**, 1933–1947.
7 Chávez,S., Candau,R., Truss,M. and Beato,M. (1995) *Mol. Cell. Biol.*, **15**, 6987–6998.
8 Truss,M., Bartsch,J., Schelbert,A., Haché,R.J.G. and Beato,M. (1995) *EMBO J.*, **14**, 1737–1751.
9 Chávez,S. and Beato,M. (1997) *Proc. Natl Acad. Sci. USA*, **94**, 2885–2890.
10 Perlmann,T. and Wrange,Ö. (1988) *EMBO J.*, **7**, 3073–3079.
11 Piña,B., Brüggemeier,U. and Beato,M. (1990) *Cell*, **60**, 719–731.
12 Roberts,M.S., Fragoso,G. and Hager,G.L. (1995) *Biochemistry*, **34**, 12470–12480.
13 Eisfeld,K., Candau,R., Truss,M. and Beato,M. (1997) *Nucleic Acids Res.*, **25**, 3733–3742.
14 Archer,T.K., Cordingley,M.G., Wolford,R.G. and Hager,G.L. (1991) *Mol. Cell. Biol.*, **11**, 688–698.
15 Peterson,C.L. and Tamkun,J.W. (1995) *Trends Biochem. Sci.*, **20**, 143–146.
16 Kwon,H., Imbalzano,A.N., Khavari,P.A., Kingston,R.E. and Green,M.R. (1994) *Nature*, **370**, 477–481.
17 Côte,J., Quinn,J., Workmann,J.L. and Peterson,C.L. (1994) *Science*, **265**, 53–59.
18 Östlund-Farrants,A.-K., Blomquist,P., Kwon,H. and Wrange,Ö. (1997) *Mol. Cell. Biol.*, **17**, 895–905.
19 Tsukiyama,T. and Wu,C. (1995) *Cell*, **83**, 1011–1020.
20 Cairns,B.R., Lorch,Y., Li,Y., Zhang,M., Lacomis,L., Erdjument-Bromage,H., Tempst,P., Du,J., Laurent,B. and Kornberg,R.D. (1996) *Cell*, **87**, 1249–1260.
21 Varga-Weisz,P.D., Wilm,M., Bonte,E., Dumas,K., Mann,M. and Becker,P.B. (1997) *Nature*, **388**, 598–602.
22 Ito,T., Bulger,M., Pazin,M.J., Kobayashi,R. and Kadonaga,J.T. (1997) *Cell*, **90**, 145–155.
23 Kingston,R.E., Bunker,C.A. and Imbalzano,A.N. (1996) *Genes Dev.*, **10**, 905–920.
24 Becker,P.B. and Wu,C. (1992) *Mol. Cell. Biol.*, **12**, 2241–2249.
25 Kamakaka,R.T., Bulger,M. and Kadonaga,J.T. (1993) *Genes Dev.*, **7**, 1779–1795.

26 Tsukiyama,T., Becker,P.B. and Wu,C. (1994) *Nature*, **367**, 525–532.
27 Pazin,M.J., Kamakaka,R.T. and Kadonaga,J.T. (1994) *Science*, **266**, 2007–2011.
28 Becker,P.B., Tsukiyama,T. and Wu,C. (1994) In Goldstein,L.S.B. and Fyrberg,E.A. (eds), *Methods in Cell Biology*, Vol 44. Academic Press Inc., San Diego, CA, pp. 207–223.
29 Carballo,M. and Beato,M. (1990) *DNA Cell Biol.*, **9**, 519–521.
30 Peck,L.J. and Wang,J.C. (1983) *Proc. Natl Acad. Sci. USA*, **80**, 6206–6210.
31 Sigman,D.S. and Chen,C.B. (1990) *Annu. Rev. Biochem.*, **59**, 207–236.
32 Cartwright,I.L., Hertzberg,R.P., Dervan,P.B. and Elgin,S.C.R. (1983) *Proc. Natl Acad. Sci. USA*, **80**, 3213–3217.
33 Meisterernst,M., Rogge,L., Donath,C., Gander,I., Lottspeich,F., Mertz,R., Dobner,T., Fîckler,R., Stelzer,G. and Winnacker,E.L. (1988) *FEBS Lett.*, **236**, 27–32.
34 Russmann,C., Stollhof,J., Weiss,R., Beigang,R. and Beato,M. (1998) *Nucleic Acids Res.*, in press.
35 Cato,A.C.B., Miksicek,R., Schütz,G., Arnemann,J. and Beato,M. (1986) *EMBO J.*, **5**, 2237–2240.
36 Keller,W. (1975) *Proc. Natl Acad. Sci. USA*, **72**, 2550–2554.
37 Nedospasov,S.A. and Georgiev,G.P. (1980) *Biochem. Biophys. Res. Commun.*, **92**, 532–539.
38 Tanaka,S., Livingstone-Zatchej,M. and Thoma,F. (1996) *J. Mol. Biol.*, **257**, 919–934.
39 Blank,T.A. and Becker,P.B. (1995) *J. Mol. Biol.*, **252**, 305–313.
40 Piña,B., Truss,M., Ohlenbusch,H., Postma,J. and Beato,M. (1990) *Nucleic Acids Res.*, **18**, 6981–8987.
41 Wall,G., Varga-Weisz,P.D., Sandaltzopoulos,R. and Becker,P.B. (1995) *EMBO J.*, **14**, 1727–1736.
42 Varga-Weisz,P.D., Blank,T.A. and Becker,P.B. (1995) *EMBO J.*, **14**, 2209–2216.
43 Längst,G., Blank,T.A., Becker,P.B. and Grummt,I. (1997) *EMBO J.*, **16**, 760–768.
44 Blomquist,P., Li,Q. and Wrange,Ö. (1996) *J. Biol. Chem.*, **271**, 153–159.
45 Simpson,R.T. (1978) *Biochemistry*, **17**, 5524–5531.
46 Blank,T.A. and Becker,P.B. (1996) *J. Mol. Biol.*, **260**, 1–8.
47 Spangenberg,C., Eisfeld,K., Stünkel,W., Luger,K., Richmonds,T.J., Truss,M. and Beato,M. (1997) *J. Mol. Biol.*, **278**, 725–739.
48 Ristiniemi,J. and Oikarinen,J. (1989) *J. Biol. Chem.*, **264**, 2164–2174.
49 Bresnick,E.H., Bustin,M., Marsaud,V., Richard-Foy,H. and Hager,G.L. (1992) *Nucleic Acids Res.*, **20**, 273–278.
50 Hayes,J.J., Pruss,D. and Wolffe,A.P. (1994) *Proc. Natl Acad. Sci. USA*, **91**, 7817–7821.
51 Pruss,D., Bartholomew,B., Persinger,J., Hayes,J., Arents,G., Moudrianakis,E.N. and Wolffe,A.P. (1996) *Science*, **274**, 614–617.
52 Hayes,J.J. (1996) *Biochemistry*, **35**, 11931–11937.
53 Beato,M. and Eisfeld,K. (1997) *Nucleic Acids Res.*, **25**, 3559–3563.
54 Li,Q. and Wrange,Ö. (1993) *Genes Dev.*, **7**, 2471–2482.
55 Li,Q. and Wrange,Ö. (1995) *Mol. Cell. Biol.*, **15**, 4375–4384.
56 Winston,F. and Carlson,M. (1992) *Trends Genet.*, **8**, 387–391.
57 Yoshinaga,S.K., Peterson,C.L., Herskowitz,I. and Yamamoto,K.R. (1992) *Science*, **258**, 1598–1604.
58 Muchardt,C. and Yaniv,M. (1993) *EMBO J.*, **12**, 4279–4290.
59 Cairns,B.R., Levinson,R.S., Yamamoto,K.R. and Kornberg,R.D. (1996) *Genes Dev.*, **10**, 2131–2144.
60 Chakravarti,D., LaMorte,V.J., Nelson,M.C., Nakajima,T., Schulman,I.G., Juguilon,H., Montminy,M. and Evans,R.M. (1996) *Nature*, **383**, 99–103.
61 Kamei,Y., Xu,L., Heinzel,T., Torchia,J., Kurokawa,R., Gloss,B., Lin,S.C., Heyman,R.A., Rose,D.W., Glass,C.K. and Rosenfeld,M.G. (1996) *Cell*, **85**, 403–414.
62 Oñate,S.A., Tsai,S.Y., Tsai,M.-J. and O'Malley,B.W. (1995) *Science*, **270**, 1354–1357.
63 Bannister,A.J. and Kouzarides,T. (1996) *Nature*, **384**, 641–643.
64 Ogryzko,V.V., Schiltz,R.L., Russanova,V., Howard,B.H. and Nakatani,Y. (1996) *Cell*, **87**, 953–959.
65 Yang,X.J., Ogryzko,V.V., Nishikawa,J., Howard,B.H. and Nakatani,Y. (1996) *Nature*, **382**, 319–324.
66 Bartsch,J., Truss,M., Bode,J. and Beato,M. (1996) *Proc. Natl Acad. Sci. USA*, **93**, 10741–10746.